Environ. Sci. Technol. **2006**, *40,* 235−242

Reduction of Nitroaromatic Compounds by Fe(II) Species Associated with Iron-Rich Smectites

THOMAS B. HOFSTETTER,*
ANKE NEUMANN, AND
RENÉ P. SCHWARZENBACH

Swiss Federal Institute of Technology (ETH) and Swiss Federal Institute for Environmental Science and Technology (EAWAG), Universitätsstr. 16, ETH Zentrum, CH-8092 Zürich, Switzerland

Reductive transformation reactions involving mineral-bound Fe^{2+} species are of great relevance for the fate of groundwater contaminants. For clay minerals, which are ubiquitously present in soils and sediments, the factors determining the reactivity of structural Fe^{2+} and surface-bound Fe^{2+} are not well understood. We investigated the reactivity and availability of Fe^{2+} species in suspensions of chemically reduced montmorillonite (SAz-1) as well as in suspensions of oxidized and reduced nontronite (SWa-1, ferruginous smectite) using two acetylnitrobenzene isomers as reactive probe compounds. The analyses of the reduction kinetics of the two nitroaromatic compounds (NACs) suggested that Fe^{2+} bound in the octahedral layer of reduced smectites is the predominant reductant and that electron transfer presumably occurs via basal siloxane planes. In contrast, reduction of NACs by Fe^{2+} associated with oxidized nontronite is orders of magnitude slower than reduction by octahedral Fe^{2+}. Reductive transformation and reversible, nonreactive electron donor−acceptor (EDA) complexation of NACs at basal smectite surfaces occur simultaneously at reduced montmorillonite exhibiting low structural iron content. In contrast, EDA complexation was not observed in suspensions of reduced iron-rich nontronite. Due to the similar reduction rate constants measured for the two NACs, we propose that the (re)-generation of octahedral Fe^{2+} sites, e.g., by electron transfer and/or Fe rearrangement within the octahedral nontronite layers, partly limited the rate of contaminant transformation. Since iron in clay minerals is available for microbial reduction, our study suggests that octahedral Fe^{2+} can contribute to abiotic contaminant transformation in anoxic environments.

Introduction

In anoxic groundwaters, biogeochemical processes provide a variety of potential reductants for abiotic contaminant transformation. Persistent organic chemicals, such as polyhalogenated alkanes and alkenes, aromatic nitro and azo compounds, may be transformed to reaction products that can be further (bio)degraded or to products that can be more toxic than the parent compounds. Reactions involving Fe^{2+} species are of great relevance for the fate of such important soil and groundwater contaminants (*1*−*4*). Therefore, an understanding of the biogeochemical processes controlling the formation and reactivity of Fe^{2+} is of particular interest for assessing the risk of subsurface contamination of drinking water resources. To date, many field and laboratory studies have shown that Fe^{2+} associated with various iron-containing minerals such as (hydr)oxides, phyllosilicates, and green rusts can efficiently reduce many different contaminants under anoxic conditions (*4*−*17*). However, even under controlled laboratory conditions, relative rates of contaminant reduction may vary over several orders of magnitude in suspensions containing Fe^{2+} bound to various iron minerals (*9*), suggesting that reduction rate constants depend on specific interactions between organic contaminant and mineral surfaces.

Among these studies, the role of clay minerals for reductive contaminant transformation by Fe^{2+} species has rarely been addressed, despite the ubiquitous presence of clay minerals in soils and sediments. Almost all clay minerals contain structural iron in the ferric and/or ferrous form, and total iron contents can be up to 25 wt % (*18*). Upon microbial reduction (*19*, *20*), Fe^{2+} species associated with clay minerals can become available for contaminant transformation. For iron-bearing smectites, we have proposed that reactive Fe^{2+} is predominantly present as Fe^{2+} bound to surface hydroxyl groups as well as structural Fe^{2+} in the octahedral layer of the minerals. The redox potential of Fe^{2+} species bound by ion exchange is presumably close to that of aqueous Fe^{2+} species and, therefore, this Fe^{2+} species is of minor significance for contaminant reduction (*15*). To assess the reactivity and reduction capacity of Fe^{2+} species associated with clay minerals in anoxic soils and groundwaters, the distinction between the predominant structural or surface associated iron species is of great importance.

However, recent studies have demonstrated that the concept of isolated reactive Fe^{2+} sites at the surface or within the mineral structure might be too limited to address the nature of reactive Fe^{2+}. At Fe^{3+}(hydr)oxides, an oxidation of surface-bound Fe^{2+} species by structural Fe^{3+} was observed in the absence of oxygen (*13*). Reduction of contaminants by surface-bound Fe^{2+} species, in contrast, could only be detected when Fe^{2+} was additionally present in solution at millimolar concentration. Obviously, some $Fe^{2+}-Fe^{3+}$ electron transfer takes place prior to the formation of reactive Fe^{2+} species and may be responsible for the (re)generation of reactivity during contaminant transformation. Therefore, comparisons of reactivity of octahedral and surface-bound Fe^{2+} associated with clay minerals need to address the influence of structural iron oxidation state on the formation of reactive Fe^{2+}.

It is the scope of this study to contribute to a better understanding of the predominant reactive Fe^{2+} species associated with oxidized and reduced iron-rich smectites with regard to their accessibility and reactivity for contaminant transformation. To this end, we examined the reactivity of Fe^{2+} associated with chemically reduced smectites in the presence and absence of surface-bound Fe^{2+} and compared our findings with the reactivity of Fe^{2+} at an oxidized, iron-rich smectite. Using montmorillonite (SAz-1, Arizona montmorillonite) and iron-rich nontronite (SWa-1, ferruginous smectite) as model smectites, we investigated (i) which reactive iron pool, octahedral Fe^{2+} or Fe^{2+} bound to surface hydroxyl groups, is the predominant reductant, (ii) whether the reactivity of surface-bound Fe^{2+} depends on the oxidation state of structural iron, and (iii) whether contaminant transformation kinetics provide evidence for the rate-limiting

---

* Corresponding author phone: +41-44 632 83 28; fax: +41 44 633 11 22; e-mail: thomas.hofstetter@env.ethz.ch.

10.1021/es0515147 CCC: $33.50

steps of reduction as well as for the localization of electron-transfer reactions at smectite surfaces.

To probe for the reactivity and accessibility of Fe^{2+} at smectites we used two acetylnitrobenzene isomers (2- and 4-acetylnitrobenzene), which were introduced in our previous study as reactive model compounds (*15*). The ortho-substituted isomer, 2-acetylnitrobenzene, which is not enriched significantly at any of the potentially reactive surface sites, was used to assess the reactivity of Fe^{2+} in the absence of specific interactions between NAC and mineral surface. In contrast, planar NACs such as 4-acetylnitrobenzene have a high affinity for siloxane oxygens and can form coplanar electron donor−acceptor (EDA) complexes at the siloxane surface of phyllosilicates (*21*, *22*). Planar nitrobenzenes can, therefore, be used to probe directly for specific interactions with octahedral Fe^{2+} via basal siloxane planes. Note that EDA complexation, which occurs within seconds, is hindered by the presence of strongly hydrated cations such as Na^+ and Ca^{2+}, whereas this effect is less pronounced in the presence of K^+ or NH_4^+ at basal siloxane planes. Therefore, reduced smectites with different cations present at the basal siloxane surfaces were used to determine the contribution of specific EDA interactions to the overall contaminant reduction.

Experimental Section

Preparation of Mineral Suspensions for Kinetic Experiments. Different types of anoxic suspensions containing reduced nontronite (ferruginous smectite, SWa-1) or reduced montmorillonite (Arizona montmorillonite, SAz-1) were prepared according to a modified citrate−bicarbonate−dithionite (CBD) procedure described earlier (see refs *15*, *23*, and Supporting Information for modifications concerning montmorillonite). Chemical reduction of nontronite or montmorillonite resulted in minerals with octahedral Fe^{2+} and Fe^{2+} adsorbed to surface hydroxyl groups. Further washing cycles with acidic solutions of either 2 M NaCl or 2 M KCl at pH 4.0 were performed in the ultrafiltration cell to remove surface-bound Fe^{2+}. The adsorption of Fe^{2+} to basal nontronite surfaces was achieved by washing the clay suspension once after reduction with 50 mL of 0.1 M $FeCl_2$ solution and three times with Nanopure water until no visible sign of orange Fe^{3+}(hydr)oxides could be observed in the filtrate outside the glovebox. Assays with ion-exchangeable Fe^{2+} were prepared with $NaHCO_3$ buffer only, or with $NaHCO_3$ buffer in the presence of 1 mM dissolved Fe^{2+}_{aq}. Suspensions of oxidized nontronite were prepared identically to their reduced counterparts, except for the addition of dithionite reductant. These assays were used for adsorption experiments. Further cation exchange with $FeCl_2$ as describe above resulted in Fe^{2+} exchanged, oxidized nontronite.

Kinetic Experiments. Kinetic experiments were initiated by the addition of methanolic acetylnitrobenzene (0.02 M) stock solution with a gastight glass syringe to clay mineral suspensions. Samples of 500 μL were withdrawn at given time intervals with a gastight glass syringe after the injection of an equal volume of Ar. Immediate filtration through 0.2 μm filters into 2 mL glass vials suitable for the HPLC autosampler stopped the reaction. The obtained samples needed no further treatment prior to HPLC analysis. All experiments were performed in triplicates.

Chemical Analyses. All samples containing acetylnitrobenzenes and reduction products were analyzed using standard reversed-phase HPLC with eluents consisting of $MeOH/H_2O$ mixtures. UV/vis detection was performed simultaneously at the absorption maxima of the acetylnitrobenzenes and the corresponding anilines as described earlier (*15*). Aqueous solutions were analyzed for dissolved Fe^{2+} with a UV/vis photospectrometer at 562 nm after complexation with FerroZine or at 512 nm after complexation with phenanthroline (*24*, *25*). Total iron content of the clay minerals was measured with the means of energy dispersive XRF on a Spectro X-LAB 2000 (Kleve), equipped with a Si(Li) detector and a Pd X-ray source. For the size fractions used in our study, we determined 12.6 and 1.0 wt % total iron content in SWa-1 and SAz-1, respectively, which are somewhat lower than the published values of 19.8 wt % (SWa-1) and 1.5 wt % (SAz-1) (*26*, *27*).

TABLE 1. Rate Constants of Acetylnitrobenzene Reduction, k_{NAC}, in Suspensions of Chemically Reduced Montmorillonite (SAz-1, 24 g L^{-1}) and Adsorption Constants of 4-$COCH_3$-NB, K_d, in the Presence of Different Exchangeable Cations at Basal Siloxane Planes[a]

	2-$COCH_3$-NB	4-$COCH_3$-NB	
exchangeable cation	k_{NAC} (h^{-1})	k_{NAC} (h^{-1})	K_d (L g^{-1})
Na^+	0.11 ± 0.01	0.40 ± 0.12	0.022 ± 0.0093
K^+	0.13 ± 0.05	0.35 ± 0.61	1.4 ± 0.40

[a] Errors represent 95% confidence interval.

Modeling. Kinetic data obtained from the experiments on the adsorption and reduction of NACs in clay mineral suspensions was modeled using Aquasim modeling software (see ref *28* and Supporting Information). Briefly, the reduction of a NAC to reaction intermediates as well as the reduction of the intermediates to aniline at the clay surface was assumed to follow pseudo-first-order kinetics. The adsorption behavior of NACs at low aqueous concentrations was described with a linear sorption isotherm with the adsorption constant K_d (*22*). Reduction rate constants, k_{NAC}, and adsorption constants were calculated for every single experiment. Experimental data on NAC disappearance and aniline formation was fitted to the kinetic model and 95% confidence intervals for k_{NAC} and K_d were calculated from at least three replicates of kinetic experiments.

Results and Discussion

Reduction and EDA Complex Formation of Acetylnitrobenzenes in Reduced Montmorillonite Suspensions. We investigated the reduction kinetics of two nitroaromatic compounds (NACs), i.e., 2- and 4-acetylnitrobenzene (2-$COCH_3$-NB and 4-$COCH_3$-NB), to probe for reactive and nonreactive interactions at smectite surfaces in suspensions of reduced montmorillonite (SAz-1). Contributions of EDA complexation to an enhanced disappearance of 4-$COCH_3$-NB from aqueous solution were assessed from the comparison of reaction kinetics in suspensions of K^+ montmorillonite, where fast and strong adsorption occurs, and in the presence of the Na^+-exchanged mineral, where EDA complexation is less pronounced (*22*). Table 1 summarizes the pseudo-first-order rate constants, k_{NAC}, calculated for the reduction of the acetylnitrobenzenes ($COCH_3$-NBs) in the different experimental systems and shows the associated adsorption constants, K_d, and 4-$COCH_3$-NB.

In suspensions of reduced montmorillonite, the nonsorbing 2-$COCH_3$-NB was reduced to 2-acetylaniline following pseudo-first-order kinetics (data not shown) with a half-life of 5−6 h. The calculated rate constants for the disappearance of the acetylnitrobenzenes from aqueous solution were similar for montmorillonites exchanged with either Na^+ or K^+. As shown in Table 1, the reduction of 4-$COCH_3$-NB in suspension of Na^+- and K^+-exchanged montmorillonite was faster than the transformation of the ortho-substituted isomer, in agreement with the higher one-electron reduction potentials reported for the para-substituted NACs [E^1_h(4-$COCH_3$-NB) = −0.358 V, E^1_h(2-$COCH_3$-NB) = −0.460 V (*29*, *30*)]. However, the disappearance kinetics of 4-$COCH_3$-NB in K^+-montmorillonite suspensions were

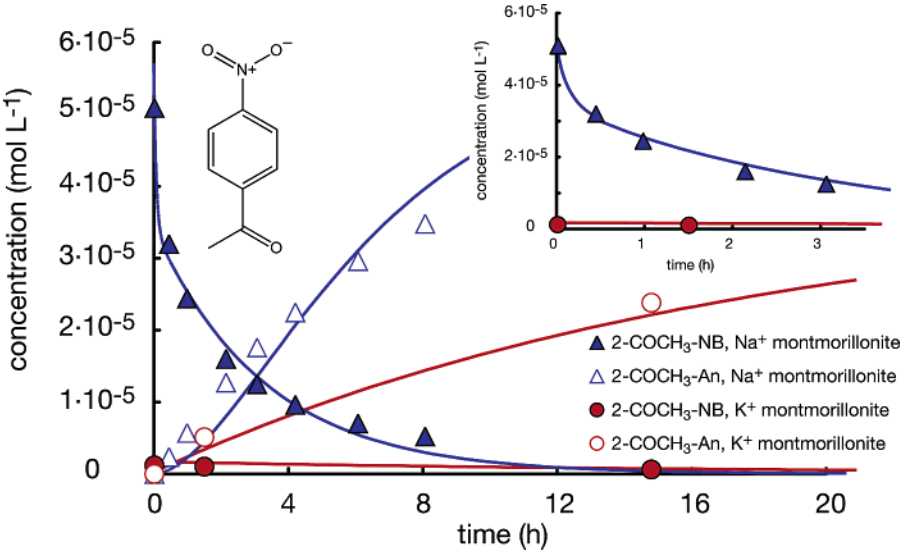

FIGURE 1. Reduction of 4-acetylnitrobenzene (4-COCH$_3$-NB) in suspensions of Na$^+$- and K$^+$-montmorillonite (SAz-1; particle concentration 24 g L^{-1}, pH 7.5) to 4-acetylaniline (4-COCH$_3$-An). Triangles and circles refer to measurements in the presence of Na$^+$- and K$^+$-montmorillonite, respectively. Initial concentrations were 57 μM (Na$^+$) and 50 μM (K$^+$). Solid lines are results of model calculations (inset: initial disappearance of 4-COCH$_3$-NB from aqueous solution due to nonreactive EDA complexation with K$^+$-montmorillonite within seconds).

significantly different from that in suspensions of Na$^+$-montmorillonite (Figure 1). The inset in Figure 1 illustrates that the initial disappearance of 4-COCH$_3$-NB from aqueous solution due to adsorption occurred within seconds and, in the presence of K$^+$-montmorillonite, to a much larger extent than in the presence of Na$^+$-montmorillonite. In suspensions of K$^+$-montmorillonite, the aqueous 4-COCH$_3$-NB concentration subsequently remained at 2 μM and the reduction product, 4-acetylaniline, was not observed until 15 min after the start of the experiment. Since no reaction intermediates such as aromatic nitroso- or hydroxyl amino compounds where detected during HPLC analyses, these observations suggest that fast, nonreactive EDA complexation enriched 4-COCH$_3$-NB at the basal siloxane surfaces, limited its aqueous concentration, and, thus, decreased the rate of aniline formation at reactive surface sites.

To test our hypothesis, we quantified the extent of EDA complexation in terms of adsorption constants that characterize the affinity of 4-COCH$_3$-NB to basal siloxane surfaces of reduced montmorillonite (*21*). We calculated the kinetic parameters of 4-COCH$_3$-NB adsorption from the initial kinetic data points (Supporting Information). Subsequently, the entire data set for 4-COCH$_3$-NB and aniline concentrations was used to calculate k_{NAC} and K_{d}. Rate constants of 4-COCH$_3$-NB reduction were similar for Na$^+$ and K$^+$-montmorillonite, as was observed for 2-COCH$_3$-NB. Since exchangeable cations did not show an effect on k_{NAC}, reactive Fe^{2+} species associated with reduced montmorillonite are presumably bound to surface sites where cation binding is irrelevant or where the accessibility of reactive Fe^{2+} is not cation sensitive. Furthermore, EDA complexation retards the formation of 4-acetylaniline, suggesting that EDA interactions do not facilitate the access to reactive Fe^{2+} species at basal siloxane surfaces. The K_{d} values (Table 1) show that the tendency of 4-COCH$_3$-NB to form EDA complexes was 2 orders of magnitude higher for K$^+$-montmorillonite than for the Na$^+$-exchanged mineral. Similar results were obtained for oxidized montmorillonites, where EDA complex formation is strongest if weakly hydrated cations such as K$^+$ are present, but almost negligible if strongly hydrated cations such as Na$^+$ are adsorbed (*21*, *22*, *31*).

Our findings obtained in suspensions of reduced montmorillonite confirm our hypothesis that nonplanar NACs such as 2-COCH$_3$-NB can be used to probe for reactivity of Fe^{2+}, whereas planar NACs such as 4-COCH$_3$-NB can undergo reductive transformation and EDA complexation simultaneously. Although k_{NAC} of 4-COCH$_3$-NB is independent of the adsorbed cation, the rate of the reduction is, in fact, strongly cation dependent. Since the rate of the reaction depends not only on the rate constant but also on the aqueous 4-COCH$_3$-NB concentration, nonreactive EDA complexation retards the overall reduction of 4-COCH$_3$-NB in suspension containing montmorillonite exchanged with weakly hydrated cations. Furthermore, the cation-dependent 4-COCH$_3$-NB adsorption is presumably indicative of specific EDA interactions of the compound at basal surfaces of oxidized and reduced montmorillonites.

Reduction of Acetylnitrobenzenes by Octahedral Fe^{2+} and Fe^{2+} Surface Complexes in Reduced Nontronite Suspension. To compare the reactivity of octahedral Fe^{2+} with that of Fe^{2+} species complexed to surface hydroxyl groups of nontronite (SWa-1, ferruginous smectite), three types of reduced mineral suspensions were prepared (see Table S1 of the Supporting Information for an overview of the different experimental systems). Suspensions of chemically reduced, i.e., CBD-treated, nontronite were homoionized with three different electrolytes, yielding nontronites with Na$^+$, K$^+$, or Fe^{2+} as exchangeable cation at the basal siloxane surface. The suspensions are henceforth denoted as Na$^+$-, K$^+$-, and Fe^{2+}-nontronite, respectively. In suspensions of Na$^+$- or K$^+$-nontronite, Fe^{2+} species were present as octahedral Fe^{2+} and as Fe^{2+} bound to surface hydroxyl groups. Further cation exchange of reduced Na$^+$-nontronite with FeCl$_2$ solutions provided suspensions of Fe^{2+}-nontronite with additional Fe^{2+} species bound by ion exchange.

To assess the reactivity of the various Fe^{2+} species, we examined the kinetics of 2-COCH$_3$-NB reduction to 2-acetylaniline at pH 7.5. Note that the reaction of 2-COCH$_3$-NB with dissolved Fe^{2+} as hydroxo or carbonato species (*12*, *32*) is negligible and that, in all experiments, reactivity is associated with the presence of solid phase only (*15*). Typical concentration time courses for the different experiments are shown in Figure 2. Reaction intermediates observed during HPLC analyses, presumably partially reduced acetylnitrobenzenes, were all quantitatively converted to 2-acetylaniline by the end of the experiments. The reduction of 2-COCH$_3$-NB by Fe^{2+} in Na$^+$-exchanged nontronite was fast and stoichiometric formation of aniline was observed within 12 h. Almost identical reactivity was found when nontronite suspensions

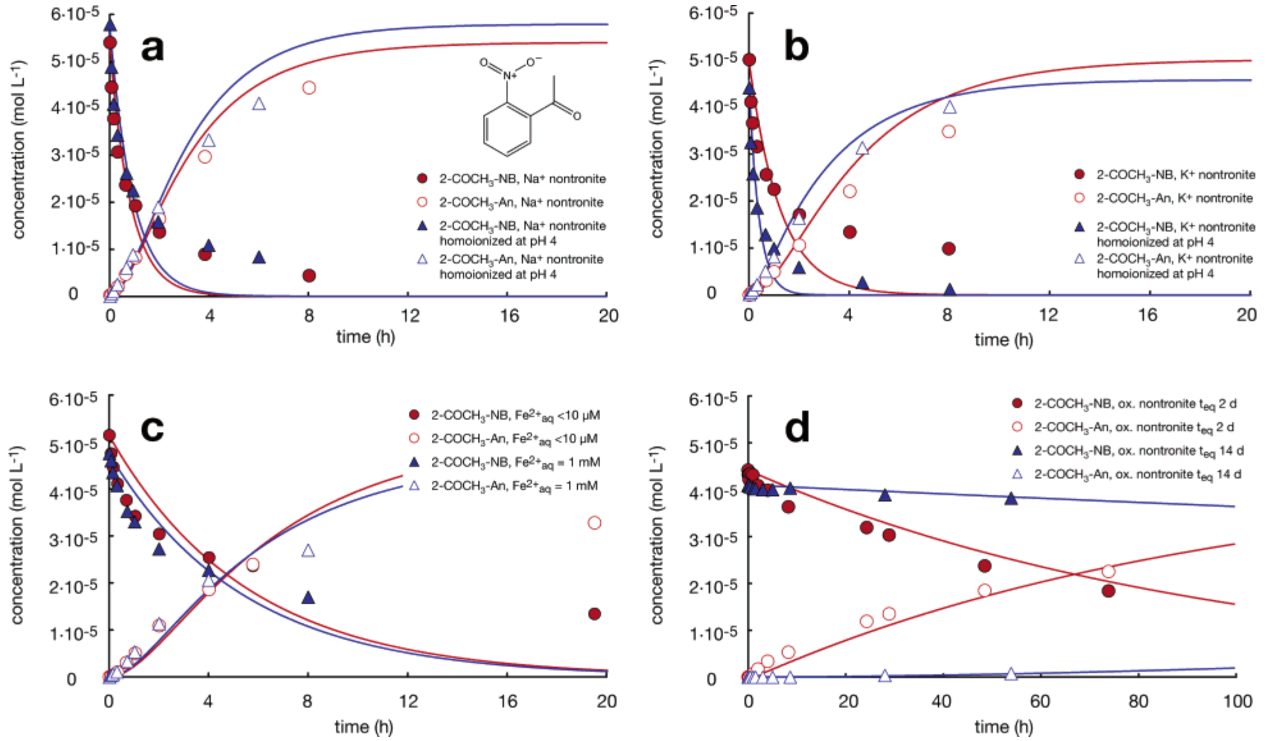

FIGURE 2. Reduction of 2-COCH$_3$-NB (filled symbols) in suspensions of reduced and oxidized nontronite (SWa-1; particle concentration 1.25 g L^{-1}) to 2-acetylaniline (2- COCH$_3$-An, open symbols) at pH 7.5: (a) reduced Na$^+$-nontronite homoionized at pH 7 (circles) and pH 4 (triangles), respectively; (b) reduced K$^+$-nontronite homoionized at pH 7 (circles) and pH 4 (triangles), respectively; (c) reduced Fe^{2+}-nontronite homoionized with FeCl$_2$ at pH 7 at [Fe$^{2+}_{aq}$] <10 μM (circles) and [Fe$^{2+}_{aq}$] = 1 mM (triangles), respectively; (d) oxidized nontronite homoionized with FeCl$_2$ at pH 7 after 2 days (circles) and 14 days (triangles) of equilibration time. The initial 2-COCH$_3$-NB concentration corresponds to the first aqueous concentration measurement. Solid lines are results of model calculations.

were washed with mildly acidic NaCl at pH 4.0 to remove Fe^{2+} bound by surface complexation (*33*) before the start of the kinetic experiment (Figure 2a). This result suggests that the removed, surface-bound Fe^{2+} species were not involved in the reduction of 2-COCH$_3$-NB. According to the nontronite treatment with acidic electrolyte, we removed approximately 130 μmol of Fe^{2+}/g of mineral from the mineral surface (see Table S2 of the Supporting Information for electron balances). Assuming that titrations down to pH 4 do not dissolve structural iron (*33*), this estimate is in good agreement with the amount of Fe^{2+} dissolved and readsorbed at the nontronite surface due to CBD treatment (*34*). However, 240 μmol of electrons/g of mineral are necessary to completely reduce 50 μM of the acetylnitrobenzene to the corresponding aniline, which cannot be accomplished exclusively by surface-bound Fe^{2+} species. Given that the acidic exchange procedure removes potentially reactive Fe^{2+} surface complexes (*33*, *35*), it is likely that octahedral Fe^{2+} species were the predominant reductants present in our suspensions. The use of an alternative Fe^{2+} extraction method, that is the exchange of Fe^{2+} for Ca^{2+}, which desorbed 44 μmol e$^-$ g^{-1}, confirms the finding that surface bound Fe^{2+} cannot account for the observed complete acetylnitrobenzene reduction. The model used for the evaluation of the kinetic data described the acetylnitrobenzene disappearance and acetylaniline formation reasonably well for aqueous concentrations above 15 μM. Since the reduction kinetics of neutral and slightly acidic washed Na$^+$-nontronite were almost identical, it is unlikely that the biphasic reduction kinetics were caused by the sequential oxidation of surface-bound and octahedral Fe^{2+}, respectively.

A similar observation with regard to the availability of surface bound vs octahedral Fe^{2+} was made for K$^+$-exchanged nontronites (Figure 2b). A comparison of the rates of 2-COCH$_3$-NB disappearance and 2-acetylaniline formation in Figure 2, parts a (Na$^+$) and b (K$^+$), further illustrates that both cations had either a similar or only a very minor influence on the reaction kinetics. We observed a different rate of 2-COCH$_3$-NB reduction in suspensions of K$^+$-nontronite before and after the acidic washing procedure. Since acid-washed minerals reacted faster with 2-COCH$_3$-NB, Fe^{2+} bound to surface hydroxyl groups was not relevant during the time scales of our experiments. However, the washing procedure might have increased the accessibility of reactive octahedral Fe^{2+}, e.g., by partially dissolving edge surfaces of nontronite (*33*) and, thus, decreasing the overall reduction capacity of the suspension (Table S2, Supporting Information).

To analyze the role of Fe^{2+} species bound electrostatically by ion exchange at the basal siloxane surfaces, the suspension of reduced nontronite was exchanged with FeCl$_2$ electrolyte. Kinetic experiments were performed in the presence and absence of dissolved Fe$^{2+}_{aq}$ to check whether the presence of aqueous Fe^{2+} is a prerequisite for reactive, surface-bound Fe^{2+} as in suspensions containing iron (hydr)oxides (*6*, *13*, *14*). Aqueous ferrous iron concentration limits were operationally defined as [Fe$^{2+}_{aq}$] = 1 mM and [Fe$^{2+}_{aq}$] < 10 μM, respectively. A comparison of Figure 2a–c shows that the reactivity of the assays was significantly lower in the presence of Fe^{2+} at the basal siloxane surfaces. The pseudo-first-order kinetic model described the initial reaction reasonably well, but the reactivity of the assays decreased significantly 6 h after the start of the experiment. The initial pseudo-first-order rate constants were very similar for experiments in the presence and absence of dissolved Fe$^{2+}_{aq}$, i.e., k_{NAC} were 0.10 and 0.16 h^{-1}, respectively. These initial rate constants were approximately 1 order of magnitude lower than those obtained for Na$^+$- and K$^+$-exchanged nontronite (k_{NAC} = 1.4 and 2.8 h^{-1}, respectively). Note that k_{NAC} values calculated from different nontronite reduction batches should only be compared on an order of magnitude basis, since the octahedral Fe^{2+} content of the different batches was not

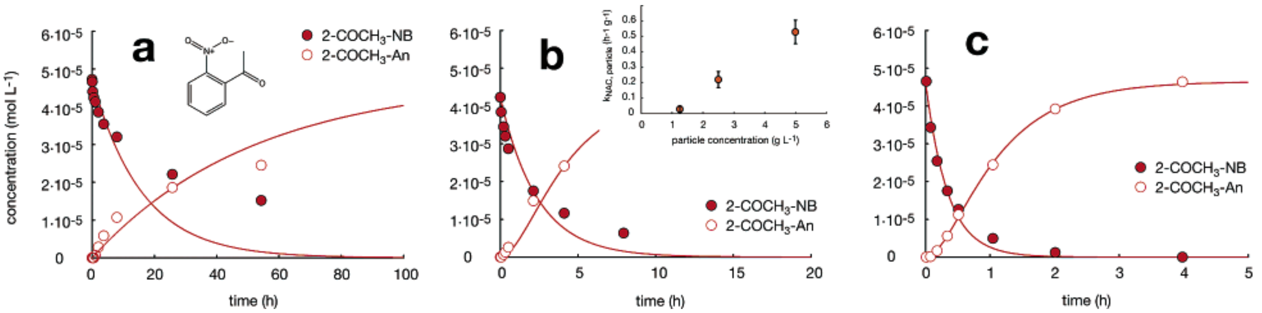

FIGURE 3. Reduction of 2-COCH$_3$-NB in suspensions of K$^+$-nontronite (pH 7.5) to 2-acetylaniline (2-COCH$_3$-An) at particle concentrations of (a) 1.25 g L^{-1}, (b) 2.5 g L^{-1}, and (c) 5 g L^{-1}. Note the different time scales of the kinetic experiments. The initial 2-COCH$_3$-NB concentration corresponds to the first concentration measurement. Solid lines are results of model calculations. The inset in part b shows particle concentration normalized rate constants, $k_{NAC,particle}$, in h^{-1} g^{-1}; error bars represent 95% confidence intervals.

measured. Although the CBD procedure was carried out under identical conditions for all experiments, minor deviations of initial rate constants due to variations in octahedral Fe^{3+} and Fe^{2+} contents cannot be ruled out completely.

On the basis of the k_{NAC} values as measures for the reactivity of Fe^{2+} species associated with reduced nontronite, the observed differences suggest that the presence of electrostatically bound Fe^{2+} reduced the reactivity of the suspensions. This finding can be due to the low reactivity found previously for Fe^{2+} bound by ion exchange (*15*). One can assume that electrostatic bonding does not lower the reduction potential compared to aqueous Fe^{2+}, as it is observed by the oxygen ligands of surface complexes (*36*). More likely, the presence of electrostatically bound Fe^{2+} limits the access of 2-COCH$_3$-NB to reactive surface sites where electron transfer from octahedral Fe^{2+} species can occur. Since (aqueous) Fe^{2+} can be expected to exchange any remaining Na^+ at the basal siloxane surfaces after chemical reduction, the reduced rate of acetylnitrobenzene reduction represents indirect evidence of an electron transfer occurring at basal siloxane surfaces.

pH Dependence. Further evidence for the importance of octahedral Fe^{2+} was obtained from the analysis of the pH dependence of the acetylnitrobenzene reduction kinetics between pH 6.5 and 8.0. Reactions involving Fe^{2+} surface complexes show strong pH dependence, since the portion of reactive Fe^{2+} hydroxo complexes as well as the amount of adsorbed Fe^{2+} increases at higher pH (*12*, *37*). Kinetic experiments with 2-COCH$_3$-NB in suspensions of Na^+-nontronite were carried out in zwitterionic buffers at pH values between 6.5 and 8.0. Despite the presence of some Fe^{2+} bound to surface hydroxyl groups at reduced nontronite, the rate constants of 2-COCH$_3$-NB reduction were almost identical for all suspension pHs (Figure S1, Supporting Information). This is in strong contrast to rate constants of nitrobenzene reduction by Fe^{2+} surface complexes at magnetite surfaces, which vary over 3 orders of magnitude for the same pH range (*6*). Since a pronounced pH effect is indicative for the abundance and thus reactivity of Fe^{2+} surface complexes, its absence in reduced nontronite suspension points out that these Fe^{2+} species were not reactive in our assays.

Effects of Particle Loadings and Initial Acetylnitrobenzene Concentration. Figure 2a–c shows that the reduction of 2-COCH$_3$-NB does not follow pseudo-first-order kinetics over the entire concentration range. Since contributions of Fe^{2+} bound by surface hydroxyl groups have been ruled out, other factors such as accessibility constraints to octahedral Fe^{2+} and/or intermolecular competition may have determined the reduction kinetics.

To investigate these effects further, experiments with different initial 2-COCH$_3$-NB to nontronite ratios were carried out. We found that at constant particle concentration, reduction rate constants, k_{NAC}, were almost independent of the initial 2-COCH$_3$-NB concentration with an average k_{NAC} of approximately 1.5 h^{-1} (Figure S2, Supporting Information). At 10 μM initial concentration, we observed an increased k_{NAC}, but 95% confidence intervals were rather large. Due to very similar rate constants obtained for initial concentrations between 20 and 180 μM, interspecies competition (*38*) for reactive sites is negligible. The higher reactivity at the lowest initial 2-COCH$_3$-NB concentration may be explained by the presence of sites with differing reactivity. At initial concentrations below 10 μM, the number of very reactive sites may not be limited, whereas above this initial concentration less reactive sites increasingly contribute to the overall acetylnitrobenzene reduction. Thus, the deviations from the pseudo-first-order kinetics after 2–4 h of reaction (Figure 2a–c) are likely to be caused by a change of the average site reactivity. This observation is corroborated by the reduction kinetics measured at constant initial 2-COCH$_3$-NB concentration but variable particle concentrations (Figure 3). At the highest nontronite concentration (5 g L^{-1}), the complete 2-COCH$_3$-NB reduction can be described by one rate constant, whereas at low and intermediate particle concentrations (1.25 and 2.5 g L^{-1}), deviations from the pseudo-first-order model become obvious. We found that rate constants normalized to the clay content of the assay ($k_{NAC,particle}$, inset Figure 3) increase with increasing bulk particle concentration. In agreement with the negligible concentration dependence of k_{NAC}, this observation reflects the limited availability of very reactive Fe^{2+} sites at high 2-COCH$_3$-NB to nontronite ratios. With increasing particle concentration, particle-normalized rate constants should become independent of the nontronite content of the suspensions.

Reactivity of Fe^{2+} Associated with Oxidized Nontronite. In another set of experiments, nontronite was treated with citrate–bicarbonate (CB) buffer, but without addition of dithionite reductant. The resulting suspension was exchanged with $FeCl_2$ solution to allow for the formation of potentially reactive Fe^{2+} surface species. With these assays, we investigated whether the presence of structural Fe^{3+} increases the reactivity of surface-bound Fe^{2+}, since the reactivity of Fe^{2+} associated with iron-free hectorite was previously found to be almost negligible (*15*). Furthermore, these experiments could indicate whether Fe^{2+} at iron-rich smectites exhibits a similar reactivity as Fe^{2+} at iron oxide surfaces (*6*–*8*, *13*, *14*).

Experiments with CB-treated, oxidized nontronite showed that 2-COCH$_3$-NB can be reduced to the corresponding aniline by surface-bound Fe^{2+}. As is shown in Figure 2d, however, the reactivity is orders of magnitude lower than for Na^+-, K^+-, or Fe^{2+}-exchanged reduced nontronites and k_{NAC} did not exceed 1.1×10^{-2} h^{-1}. Moreover, we found a further decline of reactivity when the assays containing Fe^{2+}-exchanged, oxidized nontronite were stored for up to 2 weeks

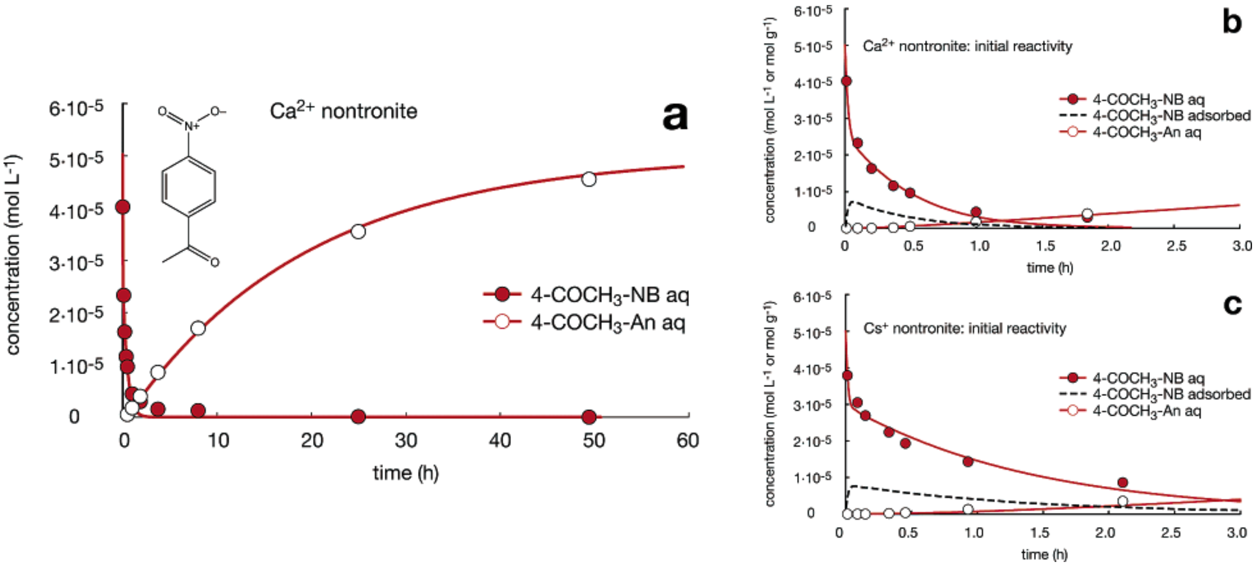

FIGURE 4. Reduction of 4-COCH$_3$-NB in suspensions of reduced Ca^{2+}- and Cs^{+}-nontronite (SWa-1, 2.5 g L^{-1}, pH 7.5) to 4-acetylaniline (4-COCH$_3$-An): (a) Ca^{2+}-nontronite, (b) Ca^{2+}-nontronite, initial reaction, (c) Cs^{+}-nontronite, initial reaction. Solid and dashed lines are results of model calculations for the concentrations of aqueous 4-COCH$_3$-NB, aqueous 4-COCH$_3$-An, and sorbed 4-COCH$_3$-NB, respectively.

before the start of kinetic experiments. Rate constants k_{NAC} were 1.2×10^{-3} h^{-1} (Figure 2d), i.e., approximately 3 orders of magnitude lower than found in reduced nontronite suspensions. In the absence of dissolved Fe$^{2+}{}_{\mathrm{aq}}$, we observed a transient color change of the suspensions from olive green to blue-green immediately after exchange of CB-treated nontronite with FeCl$_2$ electrolytes. The highest rates of 2-COCH$_3$-NB reduction were found for blue-green suspensions. At longer equilibration times, however, the color of the suspensions changed back to olive green and reduction rates decreased significantly. Since the formation of a blue-green suspension is characteristic for the presence of Fe^{2+}−O−Fe^{3+} groups within the octahedral layer of smectites (*39*), we hypothesize that these groups were formed within the first hours after treatment of the nontronite with FeCl$_2$ electrolyte. This would be consistent with recent spectroscopic findings on Fe^{2+} adsorption mechanisms at smectites (*40*, *41*), which suggest that Fe^{2+} can replace octahedral cations such as Mg^{2+} at the clay edge surfaces to form reactive Fe^{2+} species. The color changes observed over the two-week period, however, indicate that the concentration of Fe^{2+}−O−Fe^{3+} groups formed by Fe^{2+} adsorption in the anoxic suspensions must have decreased at longer equilibration times prior to the addition of 2-COCH$_3$-NB. On the basis of our experiments, it remains unclear whether processes such as migration of Fe^{2+} species in the octahedral layer (*42*, *43*) and/or Fe^{2+}−Fe^{3+} electron exchange as observed for Fe^{2+} adsorbed to ferric (oxy)hydroxides (*13*) are responsible for the formation of less reactive Fe^{2+}−O−Fe^{3+} arrangements within the smectites. Unfortunately, the rates of the hypothesized processes in nontronites are not known, and further experimental evidence is required to assess their relevance. Our preliminary findings on the reactivity of Fe^{2+} associated with oxidized nontronite, however, suggest that Fe^{2+} adsorption to iron-rich smectites may contribute to the formation of reactive Fe^{2+} surface species similar to what was found for iron(hydr)oxides (*6*, *14*, *44*).

Effects of EDA Complexation on Acetylnitrobenzene Reduction in Reduced Nontronite Suspension. To investigate the effects of electron donor−acceptor interactions of acetylnitrobenzene at basal siloxane surfaces on the accessibility of reactive Fe^{2+} species associated with reduced nontronite, a series of experiments was performed with 4-COCH$_3$-NB. In assays containing Na^{+}-, K^{+}-, or Fe^{2+}-exchanged, reduced nontronite we found the identical kinetic behavior as reported for 2-COCH$_3$-NB (Figure 2). Rates of reduction were very similar in Na^{+}- and K^{+}-nontronite suspensions but significantly slower in the presence of Fe^{2+} as exchangeable cation. These findings confirm the conclusions drawn above on the predominance of octahedral Fe^{2+} as active reductant in suspension of reduced nontronite. However, the similar behavior of 4-COCH$_3$-NB in the presence of Na^{+} as well as K^{+} as basal cations does not match the observations made with reduced montmorillonite (Figure 1) and suggests that EDA complexation did not occur. To verify this conclusion, further experiments with reduced nontronite in the presence of alternative basal cations such as Cs^{+} and Ca^{2+} were carried out. Due to the presence of Ca^{2+}, the carbonate buffer concentration was lower in these experiments to avoid precipitation of carbonates, and a series of additional kinetic experiments was performed in suspensions of Na^{+}-, K^{+}-, Cs^{+}-, or Ca^{2+}-exchanged reduced nontronite.

Typical kinetics of 4-COCH$_3$-NB reduction in Ca^{2+}-nontronite suspension are shown in Figure 4a. The disappearance of 4-COCH$_3$-NB was very fast and led to the formation of reaction intermediates, which were quantitatively transformed into 4-acetylaniline. As is shown in Figure 4b,c for the initial phase of the reaction in Ca^{2+}- and Cs^{+}-nontronite suspensions, 4-COCH$_3$-NB concentrations decreased similarly, despite the considerably different hydration energies of the cations. The reaction kinetics were almost identical in the presence of other exchangeable cations at the basal siloxane surface (Na^{+}, K^{+}, Cs^{+}, or Ca^{2+}) and, therefore, are not shown here. Sorbed 4-COCH$_3$-NB concentration was generally small, i.e., below 8 μmol 4-COCH$_3$-NB/g of nontronite, which corresponds to a K_{d} value of around 0.3 L g^{-1} (Table 2). From the observations made in K^{+}-montmorillonite suspension (Figure 1, Table 1), a stronger influence of EDA complexation of 4-COCH$_3$-NB at Cs^{+}- and K^{+}-nontronite on the reduction kinetics was expected. The absence of cation-dependent EDA complexation on the transformation kinetics at reduced nontronite surfaces, however, suggests that these interactions did not occur in our experiments.

Adsorption experiments with 4-COCH$_3$-NB in suspensions of oxidized, CB-treated K^{+}- and Na^{+}-nontronite showed that EDA complexation can occur at nontronite surfaces. Under the conditions chosen for kinetic experiments, significant 4-COCH$_3$-NB adsorption to oxidized nontronite occurred within seconds (data not shown) and adsorption constants,

TABLE 2. Rate Constants of Acetylnitrobenzene Reduction, k_{NAC}, in Suspensions of Chemically Reduced Nontronite (SWa-1, 2.5 g L^{-1}, pH 7.5) and Adsorption Constants of 4-$COCH_3$-NB, K_d, in the Presence of Different Exchangeable Cations at Basal Siloxane Planes[a]

exchangeable cation	2-$COCH_3$-NB k_{NAC} (h^{-1})	4-$COCH_3$-NB k_{NAC} (h^{-1})	4-$COCH_3$-NB K_d (L g^{-1})
Reduced Nontronite			
Na^+	1.9 ± 0.26	7.5 ± 0.70	0.27 ± 0.041
Ca^{2+}	1.5 ± 0.04	4.5 ± 0.52	0.27 ± 0.019
K^+	0.68 ± 0.094	2.6 ± 0.52	0.33 ± 0.051
Cs^+	0.62 ± 0.099	1.0 ± 0.30	0.29 ± 0.033
Oxidized Nontronite			
Na^+			0.17 ± 0.026
K^+			2.4 ± 0.81

[a] Errors represent 95% confidence interval.

K_d, were 0.17 and 2.4 L g^{-1} for Na^+- and K^+-nontronite, respectively (Table 2). This observation suggests that the effect of exchangeable cations is obvious for 4-$COCH_3$-NB adsorption at CB-treated nontronite, but the influence of cation hydration energy is less pronounced for nontronite than for montmorillonite. Furthermore, we can rule out that the absence of EDA complexation in nontronite suspensions is an artifact of our preparation procedure. At reduced nontronite, however, the effect of EDA complexation on the reduction kinetics of acetylnitrobenzenes could not be observed, presumably due to the too high reactivity of octahedral Fe^{2+} and/or the stronger hydration associated with higher surface charge density (*45*, *46*).

Table 2 summarizes the reduction rate constants, k_{NAC}, for acetylnitrobenzenes calculated for the four types of assays. Higher k_{NAC} values for 4-$COCH_3$-NB are in agreement with its higher reactivity as quantified by its E^1_h (see above). Despite considerably different E^1_h, the relative reactivities for all experiments only vary within 1 order of magnitude and k_{NAC} decreases in the order Na^+- > Ca^{2+}- > K^+- ≈ Cs^+-nontronite. This sequence shows no correlation with the cations' hydration energy, similar to what was found for reduced montmorillonite. This indicates that EDA complex formation, which would have favored 4-$COCH_3$-NB adsorption in the presence of weakly hydrated cations, did not facilitate the access of 4-$COCH_3$-NB to reactive sites at the basal siloxane surfaces. Since the disappearance of 4-$COCH_3$-NB from aqueous solution in suspensions of Na^+ and Ca^{2+} nontronite (Figure 4) were not as different as observed for Na^+- vs K^+-montmorillonite (Figure 1), nonreactive adsorption of 4-$COCH_3$-NB was irrelevant in experiments with reduced nontronite. The lack of evidence for EDA complexation at reduced nontronite suggests that interactions of 4-$COCH_3$-NB with basal siloxane surfaces were always reactive and enabled electron transfer from octahedral Fe^{2+} to 4-$COCH_3$-NB. This observation contrasts the kinetics of 4-$COCH_3$-NB disappearance in suspension of reduced montmorillonite, where we propose that 4-$COCH_3$-NB reduction and nonreactive EDA complexation occur in parallel. We suggest that the relative share of reactive vs nonreactive interactions of planar NACs such as 4-$COCH_3$-NB with basal siloxane surfaces increases with octahedral Fe^{2+} content, and therefore, EDA complexation is irrelevant at the high Fe^{2+} contents of up to 0.046 g of Fe^{2+}/g of mineral as found for reduced nontronite suspensions. However, since k_{NAC} of the two $COCH_3$-NB isomers are on the same order of magnitude, we propose that the electron transfer from an octahedral Fe^{2+} to the contaminant was not entirely rate limiting and that the (re)generation of reactive octahedral sites may have contributed to the observed rate constants.

Factors Determining the Rates of Electron Transfer in Reduced Smectites. Evidence for electron transfer via basal planes and Fe rearrangement during octahedral Fe reduction/oxidation in smectites was obtained from spectroscopic studies (*39*, *42*, *43*, *47*−*49*). Investigation of absorption bands for Fe^{2+}−Fe^{3+} intervalence electron transfer led to the conclusion that Fe^{3+} is reduced in a way that Fe ions must occupy adjacent octahedral sites and must be of different valence (*39*, *49*). As a consequence, Fe^{2+}−O−Fe^{2+} entities do not begin to form before all Fe^{3+}−O−Fe^{3+} groups are partly reduced to Fe^{2+}−O−Fe^{3+}. These observations were pivotal to the hypothesis that electron transfer to/from octahedral iron occurs via basal siloxane planes. Further studies indicated that Fe^{3+} reduction causes the migration of Fe^{2+} in the octahedral layer to form trioctahedral Fe^{2+} clusters (*42*, *43*). It is likely that in our experiments with reduced nontronites, electron transfer and the associated Fe migration occurred as proposed in the literature and, thus, partly determined the rate of $COCH_3$-NB reduction. Furthermore, the preferential formation of Fe^{2+}−O−Fe^{3+} groups suggests that surface sites of different reactivity can exist since the oxidation Fe^{2+}−O−Fe^{2+} entities would be favored compared to that of Fe^{2+}−O−Fe^{3+} sites (*39*, *49*). This is in agreement with our observation on the reduction kinetics at different $COCH_3$-NB to nontronite ratios. Thus, we assume that the Fe content as well as the distribution and arrangement of Fe^{2+} and Fe^{3+} in the octahedral layer determine the reactivity of octahedral Fe^{2+} in iron-rich smectites such as nontronite. Additional studies are necessary to address the issue of octahedral iron reactivity in smectites with measurements of Fe^{2+} reactivity at variable Fe^{2+} to Fe^{3+} ratios in minerals with different total structural iron contents. Together with an investigation of the iron reactivity in microbially reduced iron-bearing smectites, such work can contribute to future assessments of in situ generated reactive Fe^{2+} species with regard to their reactivity toward transformation of organic and inorganic contaminants.

Acknowledgments

This work was supported by ETH research grant TH-37/04-3. We acknowledge Kurt Barmettler, Soil Chemistry/ETH Zürich, for total Fe measurements and James E. Amonette, Sam J. Arey, and Timothy J. Grundl for helpful discussions and for reviewing the manuscript.

Supporting Information Available

Description of the smectite preparation and modeling procedures, two Figures and two Tables supporting the kinetic analyses of the acetylnitrobenzene reduction. This material is available free of charge via the Internet at http://pubs.acs.org.

Literature Cited

(1) Christensen, T. H.; Kjeldsen, P.; Bjerg, P. L.; Jensen, D. L.; Christensen, J. B.; Baun, A.; Albrechtsen, H. J.; Heron, C. Biogeochemistry of landfill leachate plumes. *Appl. Geochem.* **2001**, *16*, 659−718.

(2) Kenneke, J. F.; Weber, E. J. Reductive dehalogenation of halomethanes in iron- and sulfate-reducing sediments. 1. Reactivity pattern analysis. *Environ. Sci. Technol.* **2003**, *37*, 713−720.

(3) Lovley, D. R. Potential for anaerobic bioremediation of BTEX in petroleum-contaminated aquifers. *J. Ind. Microbiol. Biotechnol.* **1997**, *18*, 75−81.

(4) Rügge, K.; Hofstetter, T. B.; Haderlein, S. B.; Bjerg, P. L.; Knudsen, S.; Zraunig, C.; Mosbæk, H.; Christensen, T. H. Characterization of predominant reductants in an anaerobic leachate-affected aquifer by nitroaromatic probe compounds. *Environ. Sci. Technol.* **1998**, *32*, 23−31.

(5) Strathmann, T. J.; Stone, A. T. Mineral surface catalysis of reactions between Fe^{II} and oxime carbamate pesticides. *Geochim. Cosmochim. Acta* **2003**, *67*, 2775−2791.

(6) Klausen, J.; Tröber, S. P.; Haderlein, S. B.; Schwarzenbach, R. P. Reduction of substituted nitrobenzenes by Fe(II) in aqueous mineral suspensions. *Environ. Sci. Technol.* **1995**, *29*, 2396−2404.

(7) Amonette, J. E.; Workman, D. J.; Kennedy, D. W.; Fruchter, J. S.; Gorby, Y. A. Dechlorination of carbon tetrachloride by Fe(II) associated with goethite. *Environ. Sci. Technol.* **2000**, *34*, 4606−4613.

(8) Pecher, K.; Haderlein, S. B.; Schwarzenbach, R. P. Reductive of polyhalogenated methanes by surface-bound Fe(II) in aqueous suspensions of iron oxides. *Environ. Sci. Technol.* **2002**, *36*, 1734−1741.

(9) Elsner, M.; Schwarzenbach, R. P.; Haderlein, S. B. Reactivity of Fe(II)-bearing minerals toward reductive transformation of organic contaminants. *Environ. Sci. Technol.* **2004**, *38*, 799−807.

(10) Ernstsen, V.; Binnerup, S. J.; Sørensen, J. Reduction of nitrate in clayey subsoils controlled by geochemical and microbial barriers. *Geomicrobiol. J.* **1998**, *15*, 195−207.

(11) Lee, W. J.; Batchelor, B. Reductive capacity of natural reductants. *Environ. Sci. Technol.* **2003**, *37*, 535−541.

(12) Schultz, C. A.; Grundl, T. J. pH dependence on reduction rate of 4-Cl-nitrobenzene by Fe(II)/montmorillonite systems. *Environ. Sci. Technol.* **2000**, *34*, 3641−3648.

(13) Williams, A. G. B.; Scherer, M. M. Spectroscopic evidence for Fe(II)-Fe(III) electron transfer at the iron oxide−water interface. *Environ. Sci. Technol.* **2004**, *38*, 4782−4790.

(14) Hofstetter, T. B.; Heijman, C. G.; Haderlein, S. B.; Holliger, C.; Schwarzenbach, R. P. Complete reduction of TNT and other (poly)nitroaromatic compounds under iron reducing subsurface conditions. *Environ. Sci. Technol.* **1999**, *33*, 1479−1487.

(15) Hofstetter, T. B.; Schwarzenbach, R. P.; Haderlein, S. B. Reactivity of Fe(II) species associated with clay minerals. *Environ. Sci. Technol.* **2003**, *37*, 519−528.

(16) Ilton, E. S.; Haiduc, A.; Moses, C. O.; Heald, S. M.; Elbert, D. C.; Veblen, D. R. Heterogeneous reduction of uranyl by micas: Crystal chemical and solution controls. *Geochim. Cosmochim. Acta* **2004**, *68*, 2417−2435.

(17) Szecsody, J.; Fruchter, J. S.; Williams, M. D.; Vermeul, V. R.; Sklarew, D. In situ chemical reduction of aquifer sediments: Enhancement of reactive iron phases and TCE dechlorination. *Environ. Sci. Technol.* **2004**, *38*, 4656−4663.

(18) Murad, E.; Fischer, W. R. The geobiochemical cycle of iron. In *Iron in Soils and Clay Minerals*; Stucki, J. W., Goodman, B. A., Schwertmann, U., Eds.; D. Reidel Publishing Company: Dordrecht, 1988; Vol. 217, pp 1−18.

(19) Dong, H. L.; Kukkadapu, R. K.; Fredrickson, J. K.; Zachara, J. M.; Kennedy, D. W.; Kostandarithes, H. M. Microbial reduction of structural Fe(III) in illite and goethite. *Environ. Sci. Technol.* **2003**, *37*, 1268−1276.

(20) Kostka, J. E.; Dalton, D. D.; Skelton, H.; Dollhopf, S.; Stucki, J. W. Growth of iron(III)-reducing bacteria on clay minerals as the sole electron acceptor and comparison of growth yields on a variety of oxidized iron forms. *Appl. Environ. Microbiol.* **2002**, *68*, 6256−6262.

(21) Haderlein, S. B.; Weissmahr, K. W.; Schwarzenbach, R. P. Specific adsorption of nitroaromatic explosives and pesticides to clay minerals. *Environ. Sci. Technol.* **1996**, *30*, 612−622.

(22) Haderlein, S. B.; Schwarzenbach, R. P. Adsorption of substituted nitrobenzenes and nitrophenols to mineral surfaces. *Environ. Sci. Technol.* **1993**, *27*, 316−326.

(23) Stucki, J. W.; Golden, D. C.; Roth, C. B. Preparation and handling of dithionite-reduced smectite suspensions. *Clays Clay Miner.* **1984**, *32*, 191−197.

(24) Gibbs, C. R. Characterization and application of FerroZine iron reagent as ferrous iron indicator. *Anal. Chem.* **1976**, *48*, 1197−1201.

(25) Harvey, A. E.; Smart, J. A.; Amis, E. S. Simultaneous spectrophotometric determination of iron(II) and total iron with 1,10-phenanthroline. *Anal. Chem.* **1955**, *27*, 26−29.

(26) Lear, P. R.; Stucki, J. W. Effects of iron oxidation state on the specific surface area of nontronite. *Clays Clay Miner.* **1989**, *37*, 547−552.

(27) Van Olphen, H.; Fripiat, J. J. *Data Handbook for Clay Materials and Other Non-Metallic Minerals*; 2nd ed.; Pergamon Press: Elmsford, NY, 1979.

(28) Reichert, P. Aquasim−A tool for simulation and data-analysis of aquatic systems. *Wat. Sci. Technol.* **1994**, *30*, 21−30.

(29) Schwarzenbach, R. P.; Stierli, R.; Lanz, K.; Zeyer, J. Quinone and iron porphyrin mediated reduction of nitroaromatic compounds in homogeneous aqueous solution. *Environ. Sci. Technol.* **1990**, *24*, 1566−1574.

(30) Wardman, P. Reduction potentials of one-electron couples involving free radicals in aqueous solution. *J. Phys. Chem. Ref. Data* **1989**, *18*, 1637−1755.

(31) Weissmahr, K. W.; Haderlein, S. B.; Schwarzenbach, R. P. Complex formation of soil minerals with nitroaromatic explosives and other π-acceptors. *Soil Sci. Soc. Am. J.* **1998**, *62*, 369−378.

(32) King, D. W. Role of carbonate speciation on the oxidation rate of Fe(II) in aquatic systems. *Environ. Sci. Technol.* **1998**, *32*, 2997−3003.

(33) Tournassat, C.; Greneche, J. M.; Tisserand, D.; Charlet, L. The titration of clay minerals I. Discontinuous back-titration technique combined with CEC measurements. *J. Colloid Interface Sci.* **2004**, *273*, 224−233.

(34) Stucki, J. W.; Golden, D. C.; Roth, C. B. Effects of reduction and reoxidation of structural iron on the surface charge and dissolution of dioctahedral smectites. *Clays Clay Miner.* **1984**, *32*, 350−356.

(35) Heron, G.; Crouzet, C.; Bourg, A. C. M.; Christensen, T. H. Speciation of Fe(II) and Fe(III) in contaminated aquifer sediments using chemical-extraction techniques. *Environ. Sci. Technol.* **1994**, *28*, 1698−1705.

(36) Wehrli, B. Redox reactions of metal ions at mineral surfaces. In *Aquatic Chemical Kinetics*; Stumm, W., Ed.; John Wiley & Sons: New York, 1990; pp 311−336.

(37) Charlet, L.; Silvester, E.; Liger, E. N-compound reduction and actinide immobilisation in surficial fluids by Fe(II): The surface $Fe^{III}OFe^{II}OH^{\circ}$ species, as major reductant. *Chem. Geol.* **1998**, *151*, 85−93.

(38) Arnold, W. A.; Roberts, A. L. Pathways and kinetics of chlorinated ethylene and chlorinated acetylene reaction with Fe(O) particles. *Environ. Sci. Technol.* **2000**, *34*, 1794−1805.

(39) Komadel, P.; Lear, P. R.; Stucki, J. W. Reduction and reoxidation of nontronite: Extent of reduction and reaction rates. *Clays Clay Miner.* **1990**, *38*, 203−208.

(40) Gehin, A.; Greneche, J. M.; Tournassat, C.; Charlet, L. Specific sorption of Fe(II) on synthetic montmorillonite in anoxic conditions. *Geochim. Cosmochim. Acta* **2004**, *68*, A164-A164.

(41) Tournassat, C.; Greneche, J. M.; Charlet, L. Interactions of Fe^{2+}, Zn^{2+} and H_4SiO_4 at clay/water interface: Distinguishing competitive sorption, coadsorption and surface oxidation phenomena. *Geochim. Cosmochim. Acta* **2004**, *68*, A162-A162.

(42) Manceau, A.; Lanson, B.; Drits, V. A.; Chateigner, D.; Gates, W. P.; Wu, J.; Huo, D.; Stucki, J. W. Oxidation−reduction mechanism of iron in dioctahedral smectites: I. Crystal chemistry of oxidized reference nontronites. *Am. Mineral.* **2000**, *85*, 133−152.

(43) Drits, V. A.; Manceau, A. A model for the mechanism of Fe^{3+} to Fe^{2+} reduction in dioctahedral smectites. *Clays Clay Miner.* **2000**, *48*, 185−195.

(44) Heijman, C. G.; Grieder, E.; Holliger, C.; Schwarzenbach, R. P. Reduction of nitroaromatic compounds coupled to microbial iron reduction in laboratory aquifer columns. *Environ. Sci. Technol.* **1995**, *29*, 775−783.

(45) Stucki, J. W.; Lee, K.; Zhang, L. Z.; Larson, R. A. Effects of iron oxidation state on the surface and structural properties of smectites. *Pure Appl. Chem.* **2002**, *74*, 2145−2158.

(46) Kostka, J. E.; Wu, J.; Nealson, K. H.; Stucki, J. W. The impact of structural Fe(III) reduction by bacteria on the surface chemistry of smectite clay minerals. *Geochim. Cosmochim. Acta* **1999**, *63*, 3705−3713.

(47) Hunter, D. B.; Bertsch, P. M. In-situ measurements of tetraphenylboron degradation kinetics on clay mineral surfaces by IR. *Environ. Sci. Technol.* **1994**, *28*, 686−691.

(48) Hunter, D. B.; Gates, W. P.; Bertsch, P. M.; Kemner, K. M. Degradation of tetrapheylboron at hydrated smectite surfaces studied by time-resolved IR and X-ray absorpton sepctroscopies. In *Kinetics and Mechanisms of Reactions at the Mineral/Water Interface*; Sparks, D. L., Grundl, T. J., Eds.; ACS Symposium Series No. 715; American Chemical Society: Washington, DC, 1999; Chapter 14, pp 282−300.

(49) Lear, P. R.; Stucki, J. W. Intervalence electron transfer and magnetic exchange in reduced nontronite. *Clays Clay Miner.* **1987**, *35*, 373−378.

Received for review August 1, 2005. Revised manuscript received October 14, 2005. Accepted October 14, 2005.

ES0515147